Near-UV Absorption Spectrum of the Phenoxyl Radical and Kinetics of Its Reaction with CH_3†

Kenichi Tonokura,*,‡ Teppei Ogura, and Mitsuo Koshi

Department of Chemical System Engineering, School of Engineering, The University of Tokyo, 7-3-1 Hongo, Bunkyo-ku, Tokyo 113-8656, Japan

Received: January 23, 2004; In Final Form: March 13, 2004

Cavity ring-down spectroscopy combined with pulsed laser photolysis has been used to study the near-ultraviolet absorption spectrum (375−410 nm, $\tilde{2}^2B_1 \leftarrow \tilde{X}^2B_1$ transition) of the phenoxyl radical ($C_6H_5O^\bullet$) in 10−20 Torr of nitrogen diluent at 298 K. By using a numerical fitting routine on the basis of a modeling of chemical reaction system, the absorption cross section of the phenoxyl radical was obtained, $\sigma = (7.7 \pm 2.3) \times 10^{-18}$ cm^2 molecule^{-1} (base e) at 394.4 nm. A spectrum simulation was carried out using available Franck−Condon integrals with a 400 cm^{-1} Lorentzian line width, which suggests a short-lived excited state. Time-dependent density functional theory (TD-UB3LYP/aug-cc-pVTZ) calculations supported the interpretation of the absorption band for the phenoxyl radical. The rate constant of the phenoxyl radicals with methyl radicals was derived, $k(C_6H_5O + CH_3) = (6.2 \pm 2.6) \times 10^{-11}$ cm^3 molecule^{-1} s^{-1}, at 298 K in 20 Torr of nitrogen diluent.

1. Introduction

Phenoxyl radical ($C_6H_5O^\bullet$) is an important intermediate in the high-temperature hydrocarbon combustion and low-temperature atmospheric oxidation of small aromatic compounds such as benzene and toluene, which are important constituents of automotive gasoline. In combustion systems, the phenoxyl radical is formed via the reaction of phenyl radical with oxygen molecule and decomposes into cyclopentadienyl radical and carbon monoxide. The self-reaction of the cyclopentadienyl radicals leads to the naphthalene formation. Therefore, the phenoxyl radical is an important intermediate in the formation of soot and polycyclic aromatic hydrocarbons (PAHs).[1] It has been postulated that the phenoxyl radical plays an important role in the formation of ozone and secondary organic aerosol particles in urban air.[2]

Recognition of the importance of the phenoxyl radicals has led to numerious experimental and computational studies of its spectroscopy and kinetics. Electronic absorption spectra of the phenoxyl radicals have been studied both in gas[3−9] and condensed phases[4,10−15] and discussed by several ab initio calculations.[16−21] The UV absorption spectra of the phenoxyl radical between 220 and 300 nm have been widely studied in the gas phase.[6−8] In the ultraviolet photoelectron spectroscopy study of the phenoxide, Gunion et al.[22] observed a new absorption of the phenoxyl radical at ≤1.06 eV (1170 nm). This absorption band has been assigned to the lowest excited state by quantum chemical calculations.[14,16,21,23] The visible absorption bands of the phenoxyl radical have been observed around 600 nm.[5] Yu et al.[9] measured the absorption spectrum of the phenoxyl radical using cavity ring-down spectroscopy (CRDS) in the region of 550−602 nm and studied the kinetics of the phenoxyl radical. Platz et al.[8] measured the absorption spectrum of the phenoxyl radical in the wavelength range 220−400 nm under pulse radiolysis experiments in the gas phase. Radziszewski et al.[14,15] reported transition symmetries and absorption coefficients of the phenoxyl absorptions in the entire 190−670 nm in the low-temperature argon matrices. Resonance Raman spectroscopy has been applied to gain information about molecular structure and vibrations.[24−29]

To improve our understanding of phenoxyl radical spectroscopy, we studied the near-UV absorption spectrum using cavity ring-down spectroscopy. Time-dependent density functional theory calculations were performed to support the spectroscopic work. Reaction of phenoxyl radical with methyl radicals is important in the combustion system, since the methyl radical is one of the most abundant radical species in the hydrocarbon combustion.[1] Kinetic data for the reaction of the phenoxyl radicals with methyl radicals was also examined in this study.

2. Experimental and Computational Details

All experiments were carried out by using the CRDS combined with pulsed laser photolysis in a flow reactor described in detail elsewhere.[30−33] The ring-down cavity is 0.625 m long with a pair of high reflectance mirrors (Los Gatos Research, $R > 0.9997$ at 390 nm), with a 6 m radius of curvature, a diameter of 20 mm, and a usable bandwidth of approximately ±20 nm.

The system employs two pulsed lasers. The pulsed ArF excimer laser (193.3 nm, Lambda Physik COMPex 110) was used to photolyze a suitable precursor to generate phenoxyl radicals. The photolysis laser power used was 1−5 mJ cm^{-2} per pulse. The average photon flux across the entire sample was uniform within 10%. The excimer pumped dye laser (Lambda Physik LPX 110 + Lambda Physik LPD 3002, <10 μJ pulse^{-1}) was used to probe absorption of the phenoxyl radical. The photolysis laser entered the flow cell at a right angle to the cavity and overlapped the probe laser beam at the center of the flow cell. The probe laser was injected through one of the mirrors into the cavity. The decay of photon intensity within the cavity was measured by monitoring leakage of light through

* Corresponding author. E-mail: tonokura@esc.u-tokyo.ac.jp. Fax: +81-3-5841-2119.

† Part of the special issue "Richard Bersohn Memorial Issue".

‡ Present address: Environmental Science Center, The University of Tokyo, 7-3-1 Hongo, Bunkyo-ku, Tokyo 113-0033, Japan.

10.1021/jp049664b CCC: $27.50
Published on Web 05/18/2004

TABLE 1: Absorption Cross-Sections of the Phenoxyl Radical

	calculated[a]		observed	
states	energy (10^3 cm^{-1})	oscillator strength	energy (10^3 cm^{-1})	σ(10^{-18} cm^2 molecule^{-1})
1^2B_2	8.4	0.0000	8.9[b]	
1^2A_2	18.9	0.0048	16.0[c]	0.6[d]
2^2B_1	28.8	0.0328	25.2	7.7 ± 2.3[e]
				5.0[f]
2^2A_2	36.0	0.0399	33.9	14.2[f]
				9.7[g]
				7[h]
4^2B_1	43.1	0.1624	41.8	38.2[f]
				38.7[g]
				24[h]

[a] TD-UB3LYP/aug-cc-pVTZ calculations. [b] Reference 22. [c] Reference 5. [d] In an Ar matrix. Reference 14. [e] This work. [f] Reference 8. [g] Reference 7. [h] Reference 6.

a cutoff filter (BG24A) and a diffuser with a photomultiplier tube (PMT; Hamamatsu R955) mounted behind another mirror. The output of the signal from the PMT was fed to a 500 MHz digital oscilloscope (Tektronix TDS 520C) and transferred to a personal computer (PC). The intensity decay rate was obtained by fitting the ring-down waveform to a single-exponential decay function. Absorption spectra were obtained with a spectral resolution of 0.2 cm^{-1}. Typically, ring-down waveforms were averaged over 25 laser shots for each spectral point before being transferred to the PC. The decay of the light intensity is given by the expression:

$$I(t) = I_0 \exp(-t/\tau) = I_0 \exp(-t/\tau_0 - \sigma nc(L_R/L)t)$$

Here I_0 and $I(t)$ are the intensities of light at time 0 and t, respectively. τ_0 is the empty cavity ring-down time (2 μs at 400 nm). L_R is the length of the reaction region (30 mm). L is the cavity length (0.625 m). τ is the measured cavity ring-down time. n and σ are the concentration and absorption cross section of the species of interest, and c is the velocity of light.

Gas flows were regulated by calibrated mass flow controllers (Kofloc 3650). Anisole (Aldrich, 99.9%) and phenol (Aldrich, >99.9%) were freeze−pump−thaw degassed in liquid nitrogen to remove any volatile contaminants. N_2 (Nippon Sanso, >99.9999%) at 760 Torr passed through a bubbler containing sample at room temperature. The total pressure was measured at the center of the flow cell with a capacitance manometer (MKS Baratron 622). All experiments were carried out at room temperature (298 ± 5 K). Quoted uncertainties are one standard deviation from regression analyses.

The equilibrium geometry of the ground state of the phenoxyl radical was optimized employing a hybrid density function theory B3LYP, based on Becke's three-grid integration[34] and exchange functional and the correction functional of Lee, Yang, and Parr,[35] with Dunning's correction consistent aug-cc-pVTZ basis set.[36] Electronic transitions of the phenoxyl radical were investigated employing time-dependent density functional theory (TD-DFT) calculations.[37] The calculations were based on the $^2B_1$ ground-state equilibrium.[38] C_{2v} molecular symmetry was assumed for the equilibrium geometry of the ground state. Calculations were carried out using the Gaussian 98 program package.[39] Table 1 shows the predicted electronic transitions.

3. Results and Discussion

3.1. Near-UV Absorption Spectrum in the 375−410 nm Wavelength Range. The 193.3 nm photolysis of anisole and phenol was used to record the near-UV spectrum of the phenoxyl radical. Figure 1 shows the absorption spectrum of the phenoxyl radical in the spectral region between 375 and 410 nm. The same absorption spectrum was observed with two different precursors, which is a strong evidence for the production and detection of the same spectral carrier in these systems. The absorption spectrum exhibits no fine structure within the probe laser bandwidth ($\Delta\nu$ = 0.2 cm^{-1}) and no dependence on total pressure (10−50 Torr, 1 Torr ≈ 133.322 Pa). The absorption spectra were measured by recording the initial absorbance following pulsed photolysis of the precursor molecules. The time between the photolysis and probe laser beams was 5 μs.

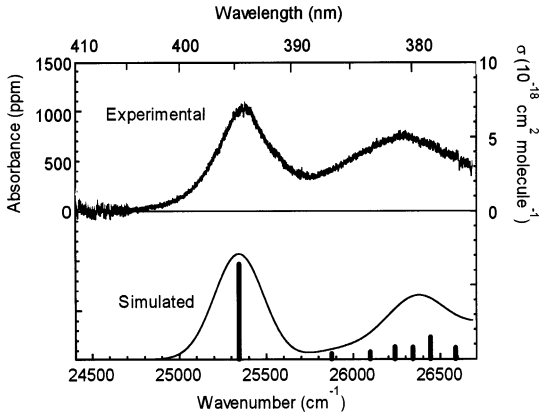

Figure 1. Experimental (top) and simulated (bottom) absorption spectra of the phenyl radical.

The typical dependences of absorbance vs photolysis laser power exhibit slopes of 1.07 ± 0.03 and 1.03 ± 0.03 for anisole and phenol, respectively, indicating that it is a one-photon absorption process. The dependences of absorbance vs precursor concentration were also unity. Multiphoton excitation of the parent molecule and secondary photodissociation of primary products are not significant. The peak positions in the spectrum agree with the electronic absorption spectrum ascribed to the phenoxyl radical with a band origin at 25 320 cm^{-1} reported by Land et al.[4] and Platz et al.,[8] indicating the production and detection of the phenoxyl radical in the present study. Takahashi et al.[19] calculated the vertical transition energy of the electronic absorption of the phenoxyl radical by MR−CI−SD calculations with the DZV basis set. The excitation energy for the $\tilde{2}^2B_1 \leftarrow \tilde{X}^2B_1$ transition was expected to be 26 340 cm^{-1}. Liu et al.[21] also calculated the vertical excitation energy of 27 142 cm^{-1} for the $\tilde{2}^2B_1 \leftarrow \tilde{X}^2B_1$ transition by state-averaged CASSCF-(9,8)/6-31G* level of theory. The present TD-UB3LYP/aug-cc-pVTZ calculations showed a vertical excitation energy of 28 800 cm^{-1} for the $\tilde{2}^2B_1 \leftarrow \tilde{X}^2B_1$ transition (Table 1). These computational results are quite close to the absorption band observed around 26 400 cm^{-1}. More recently, Radziszewski et al.[14] studied the transition symmetries from polarization measurements on photooriented samples in low-temperature argon matrices. As the transition around 400 nm was long-axis (z-axis) polarized, they assigned this absorption band to the $\tilde{2}^2B_1 \leftarrow \tilde{X}^2B_1$ transition ($\pi-\pi^*$ transition). The spectral features measured in low-temperature argon matrixes[12,14] and in an aqueous phase[11] are indistinguishable from those found in the present gas-phase spectrum.

Bottom panel of Figure 1 shows the simulated absorption spectrum for the $\tilde{2}^2B_1 \leftarrow \tilde{X}^2B_1$ transition using Franck−Condon integrals calculated by Takahashi et al.[19] The 0−0 band was adjusted to the experimental value (25 320 cm^{-1}), and the final contour was obtained by convoluting the calculated stick spectrum with a 400 cm^{-1} Lorentian line shape. This broadening of the band would be the lifetime broadening. The vibronic

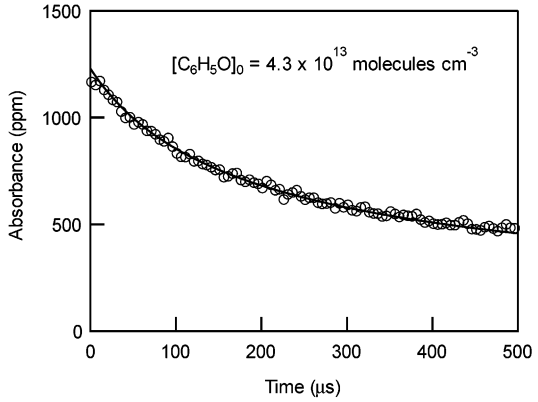

Figure 2. Decay trace of the phenoxyl radical produced in the 193.3 nm photolysis of anisole, monitoring at 394.4 nm. The solid curve is the best fit of the data.

structure of the spectrum observed experimentally is well reproduced by the calculations. This result also supports that the absorption spectrum measured in the spectral range of 375−410 nm is assigned to the $\tilde{2}^2B_1 \leftarrow \tilde{X}^2B_1$ electronic transition of the phenoxyl radical. The second absorption peak at 26 400 cm^{-1} is a convoluted band with some vibronic bands assigned to CO stretching and ring breath/CCC bending modes.[19,20]

3.2. Determination of $\sigma(C_6H_5O)$ and $k(C_6H_5O + CH_3)$. Figure 2 shows a decay trace of the phenoxyl radical absorption produced from the 193.3 nm photolysis of anisole monitored at 394.4 nm. The circles represent the absorbance of the phenoxyl radical as a function of delay time between the photolysis laser and the probe laser. The quantum yield (ϕ) of the phenoxyl radical formation following the $\pi-\pi^*$ transition of the anisole at 193.3 nm was determined to be 0.75 ± 0.15:[6]

$$C_6H_5OCH_3 + 193.3\ nm \rightarrow C_6H_5O + CH_3 \qquad (R1)$$

The main photoproducts are the phenoxyl radical and methyl radical. The initial concentrations of phenoxyl and methyl radical are the same. The initial concentration of the phenoxyl radical is estimated from the following relation:

$$[C_6H_5O]_0 = N_p[C_6H_5OCH_3]\sigma^{193}_{C_6H_5OCH_3}\phi \qquad (1)$$

where $[C_6H_5OCH_3]$ is the anisole concentration, σ is the absorption cross section of anisole ($\sigma_{C_6H_5OCH_3} = 5.4 \times 10^{-17}$ cm^2 $molecule^{-1}$ [40]), and N_p is the number density of laser photons as determined from laser pulse energy measurements. Assuming the Beer−Lambert law, the initial absorbance A_0 is given by

$$A_0 = \sigma_{C_6H_5O}[C_6H_5O]_0 L_R \qquad (2)$$

where $\sigma_{C_6H_5O}$ is the absorption cross section of the phenoxyl radical at wavelength λ and L_R is the absorption path length induced by photolysis laser beam (30 mm). In the anisole photolysis system, the time dependence of the phenoxyl concentration would be governed by the phenoxyl−phenoxyl, methyl−methyl, and phenoxyl−methyl bimolecular reactions.

$$C_6H_5O + C_6H_5O \rightarrow \text{products} \qquad (R2)$$

$$CH_3 + CH_3 + M \rightarrow \text{products} \qquad (R3)$$

$$C_6H_5O + CH_3 \rightarrow \text{products} \qquad (R4)$$

TABLE 2: Reactions Used in the Modeling of the Phenoxyl Radical Kinetics in the 193 nm Photolysis of Anisole

reaction	rate const (cm^3 $molecule^{-1}$ s^{-1})	ref
$C_6H_5OCH_3 + 193.3\ nm \rightarrow C_6H_5O + CH_3$	$\phi = 0.75 \pm 0.15$	6
$C_6H_5O + C_6H_5O \rightarrow$ products	1.2×10^{-11}	7
$CH_3 + CH_3 \rightarrow C_2H_6$	5.2×10^{-11} (20 Torr)	41
$C_6H_5O + CH_3 \rightarrow$ products	$(6.2 \pm 2.6) \times 10^{-11}$	*a*

[a] This work.

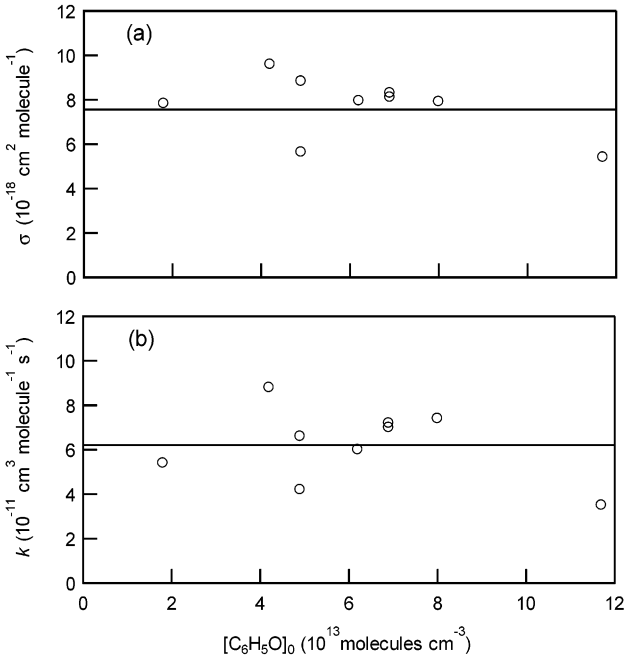

Figure 3. Plots of calculated (a) absorption cross sections of the phenoxyl radical at 394.4 nm and (b) rate constants of the reaction of the phenoxyl radical with methyl radical as a function of $[C_6H_5O]_0$ following the 193.3 nm photolysis of anisole.

Table 2 presents the reaction mechanism of the phenoxyl radicals following the 193.3 nm photolysis of anisole. Rate constants of the reactions R2 and R3 are $k_2 = 1.2 \times 10^{-11}$ cm^3 $molecule^{-1}$ s^{-1} [7] and $k_3 = 5.2 \times 10^{-11}$ cm^3 $molecule^{-1}$ s^{-1} at 20 Torr,[41] respectively. In analogy with the reaction of $C_6H_5O + C_6H_5OH$,[8] the reaction of $C_6H_5O + C_6H_5OCH_3$ would be a slow reaction. To our knowledge, the value of k_4 has never been reported.

The value of k_4 can be determined by fitting the calculated decay rates to the decay traces. Three parameters were varied simultaneously to provide the best fit; $[C_6H_5O]_0 = [X]$, k_4, and σ(394.4 nm). The values of σ and k_4 were estimated independently because of a week correlation of k_4 and σ(394.4 nm) in the curve fitting procedure. The curve in Figure 2 is fitted to the data which show that the simple model provides a good description of the experimental observations. The values of $[C_6H_5O]_0$ obtained from the curve-fitting procedure agree with those determined from eq 1, indicating no interference by minor photodissociation channels such as $C_6H_5 + OCH_3$ exists in the analysis. Figure 3 shows the results of the analyses for σ(394.4 nm) of the phenoxyl radical and $k_4(C_6H_5O + CH_3)$ as a function of $[C_6H_5O]_0$. Average values in parts a and b of Figure 3 are $\sigma(394.4\ nm) = (7.7 \pm 2.3) \times 10^{-18}$ cm^2 $molecule^{-1}$ and $k_4(C_6H_5O + CH_3) = (6.2 \pm 2.6) \times 10^{-11}$ cm^3 $molecule^{-1}$ s^{-1}, respectively. The value of $k_4(C_6H_5O + CH_3) = (6.2 \pm 2.6) \times 10^{-11}$ cm^3 $molecule^{-1}$ s^{-1} is close to the rate constant for $CH_3O + CH_3$ reaction, 2.62×10^{-11} cm^3 $molecule^{-1}$ s^{-1}.[42]

We need to consider interference by the products of recombination reactions R2−R4 in the spectroscopic and kinetic studies. The final product in the self-reaction of methyl radicals is ethane.[41] The phenoxyl radical takes the following resonance structures:

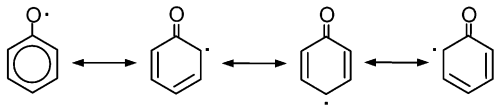

Mulliken spin densities predicted by the density functional calculations at UB3LYP/aug-cc-pVTZ level of theory are +0.42, +0.27, −0.12, and +0.36 electrons at the phenoxyl oxygen and ortho, meta, and para carbon positions, respectively. Therefore, 3! = 6 products are possible in a self-reaction of the phenoxyl radical. Platz et al. identified the major product of the self-reaction of the phenoxyl radicals as 4-phenoxylphenol (4-C_6H_5-OC_6H_4OH).[8] The rate constant of the self-reaction of phenoxyl radicals exhibits a negative temperature dependence in the temperature range of 280−423 K, $k_2 = (1.44 \pm 0.16) \times 10^{-11}$ exp[$(631 \pm 37)/T$] cm^3 molecule^{-1} s^{-1}.[7] This negative temperature dependence and the results of product analysis suggest that the self-reaction of phenoxyl radicals proceeds via an associated complex and a hydrogen atom shift:

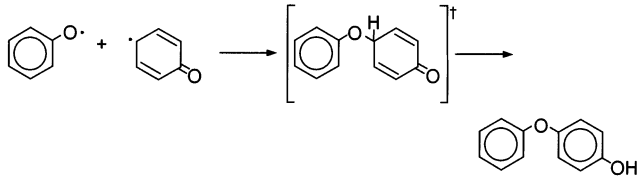

Buth et al.[43] examined the reaction pathways of $C_6H_5O + CH_3$ reaction at room temperature.

$$C_6H_5O + CH_3 \rightarrow C_6H_5OCH_3 \text{ (anisole)} \qquad \text{(R5a)}$$

$$C_6H_5O + CH_3 \rightarrow CH_3C_6H_4OH \text{ (}o\text{- or }p\text{-cresol)} \qquad \text{(R5b)}$$

The channel ratio (R5a):(R5b) of 0.59:0.41 was deduced. In higher temperature region, *o*- and *p*-cresol were detected as the main products by Mulcahy and Williams.[44,45] It has been predicted that the $C_6H_5O + CH_3$ reaction takes place via vibrationally excited cyclohexadienone intermediates (e.g., the ortho case).[9,46]

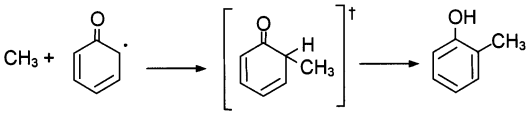

The results of the population analyses are in reasonable agreement with those of the product analyses of $C_6H_5O + C_6H_5O$ and $C_6H_5O + CH_3$ reactions. The final products of above three recombination reactions have no absorption in the near-UV region and do not interfere in the spectroscopic and kinetic studies.

Platz et al.[8] reported the absorption spectrum of the phenoxyl radical at wavelengths from 220 to 400 nm in the gas-phase. They estimated the absorption cross section of ca. 5×10^{-18} cm^2 molecule^{-1} at 394.4 nm. This result is in reasonable agreement with our value of $(7.7 \pm 2.3) \times 10^{-18}$ cm^2 molecule^{-1} within experimental errors. Radziszewski et al.[14] studied the UV and visible absorption of the phenoxyl radical in low-temperature (7 K) argon matrices. From Figure 5 in ref 14, the absorption cross-section at 394.4 nm is estimated to be 1.3×10^{-17} cm^2 molecule^{-1}. The small inconsistency between in the gas-phase and in low-temperature argon matrices may be ascribed to perturbations from argon atoms surrounding the phenoxyl radicals. Strong absorptions have been observed in the UV region. At 230 nm, the absorption band assigned to the $\tilde{4}^2B_1 \leftarrow \tilde{X}^2B_1$ transition, the absorption cross-section was well established to be 3.8×10^{-17} cm^2 molecule^{-1}.[7,8] The absorption cross section at 290 nm assigned to the $\tilde{2}^2A_2 \leftarrow \tilde{X}^2B_1$ transition has been reported to be ca. 14×10^{-18} cm^2 molecule^{-1}.[8] Oscillator strengths for the electronic transitions around 230, 290, and 400 nm are evaluated to be 0.1624, 0.0399, and 0.0328, respectively, by TD-UB3LYP/aug-cc-pVTZ calculations (Table 1). The absorption cross section in the near-UV band can be roughly estimated from the calculated oscillator strengths and the absorption cross sections in the UV absorption bands.

$$\sigma(2^2B_1) = \frac{f(2^2B_1)}{f(2^2A_2 \text{ or } 4^2B_1)}\sigma(2^2A_2 \text{ or } 4^2B_1)$$

where σ is the absorption cross section at the absorption maximum of the band and f is the oscillator strength for each transition. From the above equation, $\sigma(2^2B_1) = 11 \times 10^{-18}$ and 7.9×10^{-18} cm^2 molecule^{-1} are derived on the basis of $\tilde{2}^2A_2$ and $\tilde{4}^2B_1$ states, respectively. These values agree reasonably well with our present value, $\sigma(394.4 \text{ nm}) = (7.7 \pm 2.3) \times 10^{-18}$ cm^2 molecule^{-1}. On the basis of $\sigma(394.4 \text{ nm}) = (7.7 \pm 2.3) \times 10^{-18}$ cm^2 molecule^{-1}, the absorption cross sections in the wavelength range 375−410 nm are obtained (Figure 1). The oscillator strength of the $\tilde{1}^2A_2 \leftarrow \tilde{X}\ ^2B_1$ transition around 600 nm is predicted to be ca. one-seventh of that of the $\tilde{2}^2B_1 \leftarrow \tilde{X}^2B_1$ transition (Table 1). Using this value, an absorption cross section of the visible band around 600 nm is roughly estimated to be ca. 1×10^{-18} cm^2 molecule^{-1}. This value is consistent with the value, $\sigma(\tilde{1}^2A_2) = 0.6 \times 10^{-18}$ cm^2 molecule^{-1}, estimated by Radziszewski et al. in the argon matrices.[14]

4. Conclusions

We report herein the absolute measurement of the near-UV absorption spectrum of the phenoxyl radical in the region 375−410 nm. Our result for $\sigma(394.4 \text{ nm}) = (7.7 \pm 2.3) \times 10^{-18}$ cm^2 molecule^{-1} is in good agreement with the measurement of Plaz et al.[8] of $\sigma(394.4 \text{ nm}) \approx 5 \times 10^{-18}$ cm^2 molecule^{-1}. The diffuse character of vibronic lines on the near-UV absorption band is attributed to the lifetime broadening. Time-dependent density functional theory calculations (TD-UB3LYP/aug-cc-pVTZ) support the estimate of the absorption cross section. Phenoxyl radicals react rapidly with CH_3 with rate constant of $(6.2 \pm 2.6) \times 10^{-11}$ cm^3 molecule^{-1} s^{-1}. The absorption cross sections of the phenoxyl radical measured in the near-UV region, and the reaction rate constant of $C_6H_5O + CH_3$ reaction reported here will facilitate quantification of phenoxyl radicals in combustion and in urban atmosphere.

Acknowledgment. This work was supported in part by a Grant-in-Aid from the Ministry of Education, Science, Sports, and Culture (No. 13640502 and priority field "Radical Chain Reactions") and the Mitsubishi Chemical Corporation Fund.

References and Notes

(1) Marinov, N. M.; Pitz, W. J.; Westbrook, C. K.; Vincitore, A. M.; Castaldi, M. J.; Senkan, S. M.; Melius, C. F. *Combust. Flame* **1998**, *114*, 192.

(2) Calvert, J. G.; Atkinson, R.; Becker, K. H.; Kamens, R. M.; Seinfeld, J. H.; Wallington, T. J.; Yarwood, G., *Mechanisms of Atmospheric*

Oxidation of Aromatic Hydrocarbons; Oxford University Press: Oxford, England, 2002.

(3) Porter, G.; Wright, F. J. *Trans. Faraday Soc.* **1955**, *51*, 1469.

(4) Land, E. J.; Porter, G.; Strachan, E. *Trans. Faraday Soc.* **1961**, *57*, 1885.

(5) Ward, B. *Spectrochim. Acta* **1968**, *24A*, 813.

(6) Kajii, Y.; Obi, K.; Nakashima, N.; Yoshihara, K. *J. Chem. Phys.* **1987**, *87*, 5059.

(7) Berho, F.; Lesclaux, R. *Chem. Phys. Lett.* **1997**, *279*, 289.

(8) Platz, J.; Nielsen, O. J.; Wallington, T. J.; Ball, J. C.; Hurley, M. D.; Straccia, A. M.; Schneider, W. F.; Sehested, J. *J. Phys. Chem. A* **1998**, *102*, 7964.

(9) Yu, T.; Mebel, A. M.; Lin, M. C. *J. Phys. Org. Chem.* **1995**, *8*, 47.

(10) Roebber, J. L. *J. Chem. Phys.* **1962**, *37*, 1974.

(11) Schuler, R. H.; Buzzard, G. K. *Int. J. Radiat. Phys. Chem.* **1976**, *8*, 563.

(12) Pullin, D.; Andrews, L. *J. Mol. Struct.* **1982**, *95*, 181.

(13) Tripathi, G. N. R.; Schuler, R. H. *J. Chem. Phys.* **1984**, *81*, 113.

(14) Radziszewski, J. G.; Gil, M.; Gorski, A.; Spanget-Larsen, J.; Waluk, J.; Mroz, B. J. *J. Chem. Phys.* **2001**, *115*, 9733.

(15) Spanget-Larsen, J.; Gil, M.; Gorski, A.; Blake, D. M.; Waluk, J.; Radziszewski, J. G. *J. Am. Chem. Soc.* **2001**, *123*, 11253.

(16) Johnston, L. J.; Mathivanan, N.; Negri, F.; Siebrand, W.; Zerbetto, F. *Can. J. Chem.* **1993**, *71*, 1655.

(17) Liu, R.; Zhou, X. *J. Phys. Chem.* **1993**, *97*, 9613.

(18) Chipman, D. M.; R. Liu, R.; X. Zhou, X.; P. Pulay, P. *J. Chem. Phys.* **1994**, *100*, 5023.

(19) Takahashi, J.; Momose, T.; Shida, T. *Bull. Chem. Soc. Jpn.* **1994**, *67*, 964.

(20) Takahashi, J.; Shida, T. *Bull. Chem. Soc. Jpn.* **1994**, *67*, 2038.

(21) Liu, R.; Morokuma, K.; Mebel, A. M.; Lin, M. C. *J. Phys. Chem.* **1996**, *100*, 9314.

(22) Gunion, R. F.; Gilles, M. K.; Polak, M. L.; Lineberger, W. C. *Int. J. Mass Spectrom. Ion Processes* **1992**, *117*, 601.

(23) Hirata, S.; Head-Gordon, M. *Chem. Phys. Lett.* **1999**, *302*, 375.

(24) Beck, S. M.; Brus, L. E. *J. Chem. Phys.* **1982**, *76*, 4700.

(25) Tripathi, G. N. R.; Schuler, R. H. *Chem. Phys. Lett.* **1983**, *98*, 594.

(26) Tripathi, G. N. R.; Schuler, R. H. *J. Chem. Phys.* **1984**, *81*, 113.

(27) Johnson, C. R.; Ludwig, M.; Asher, S. A. *J. Am. Chem. Soc.* **1986**, *108*, 905.

(28) Tripathi, G. N. R.; Schuler, R. H. *J. Phys. Chem.* **1988**, *92*, 5129.

(29) Tripathi, G. N. R. In *Time-Resolved Spectroscopy*; Clark, R. J. H., Hester, R. E., Eds.; Wiley: New York, 1989; p 157.

(30) Tonokura, K.; S. Marui, S.; Koshi, M. *Chem. Phys. Lett.* **1999**, *313*, 771.

(31) Tonokura, K.; Koshi, M. *J. Phys. Chem. A* **2000**, *104*, 8456.

(32) Tonokura, K.; Norikane, Y.; Koshi, M.; Nakano, Y.; Nakamichi, S.; Goto, M.; Hashimoto, S.; Kawasaki, M.; Sulbaek Andersen, M. P.;Hurley, M. D.; Wallington, T. J. *J. Phys. Chem. A* **2002**, *106*, 5908.

(33) Tonokura, K.; Koshi, M. *J. Phys. Chem. A* **2003**, *107*, 4457.

(34) (a) Becke, A. D. *J. Chem. Phys.* **1993**, *98*, 5648. (b) Becke, A. D. *J. Chem. Phys.* **1992**, *96*, 2155. (c) Becke, A. D. *J. Chem. Phys.* **1992**, *97*, 9173.

(35) Lee, C.; Yang, W.; Parr, R. G. *Phys. Rev. B* **1988**, *37*, 785.

(36) (a) Wong, M. W.; Dunning, T. H., Jr. *J. Chem. Phys.* **1993**, *98*, 1358. (b) Kendall, R. A.; Dunning, T. H., Jr. *J. Chem. Phys.* **1992**, *96*, 6796.

(37) Koch, W.; Holthausen, M. C. *A Chemist's Guide to Density Functional Theory*; Wiley-VCH: Weinheim, Germany, 2000.

(38) *x*, *y*, and *z* axes are defined in accordance with Mulliken's recommendation, with the *y* axis in the molecular plane.

(39) Frisch, M. J.; Trucks, G. W.; Schlegel, H. B.; Scuseria, G. E.; Robb, M. A.; Cheeseman, J. R.; Zakrzewski, V. Z.; Montgomery, J. A., Jr.; Stratmann, R. E.; Burant, J. C.; Dapprich, S.; Millam, J. M.; Daniels, A. D.; Kudin, K. N.; Strain, M. C.; Farkas, O.; Tomasi, J.; Barone, V.; Cossi, M.; Cammi, R.; Mennucci, B.; Pomelli, C.; Adamo, C.; Clifford, S.; Ochterski, J.; Petersson, G. A.; Ayala, P. Y.; Cui, Q.; Morokuma, K.; Malick, D. K.; Rabuck, A. D.; Raghavachari, K.; Foresman, J. B.; Cioslowski, J.; Ortiz, J. V.; Baboul, A. G.; Stefanov, B. B.; Liu, G.; Liashenko, A.; Piskorz, P.; Komaromi, I.; Gomperts, R.; Martin, R. L.; Fox, D. J.; Keith, T.; Al-Laham, M. A.; Peng, C. Y.; Nanayakkara, A.; Gonzalez, C.; Challacombe, M.; Gill, P. M. W.; Johnson, B.; Chen, W.; Wong, M. W.; Andres, J. L.; Gonzalez, C.; Head-Gordon, M.; Replogle, E. S.; Pople, J. A. *Gaussian 98*, Revision A.7, Gaussian, Inc., Pittsburgh, PA, 1998.

(40) Kimura, K.; Nagakura, S. *J. Mol. Phys.* **1964**, *9*, 117.

(41) Slagle, I. R.; Gutman, D.; Davies, J. W.; Pilling, M. J. *J. Phys. Chem.* **1988**, *92*, 2455.

(42) Heicklen, J. *Adv. Photochem.* **1988**, *14*, 177.

(43) Buth, R.; Hoyermann, K.; Seeba, J. *25th Symp. Int. Combust.* **1994**, 841.

(44) Mulcahy, M. F. R.; Williams, D. J. *Nature (London)* **1963**, *199*, 761.

(45) Mulcahy, M. F. R.; Williams, D. J. *Aust. J. Chem.* **1965**, *18*, 20.

(46) Lin, C.-Y.; Lin, M. C. *Aust. J. Chem.* **1986**, *39*, 723.